

# Novel Ambipolar Orthogonal Donor–Acceptor Host for Blue Organic Light Emitting Diodes

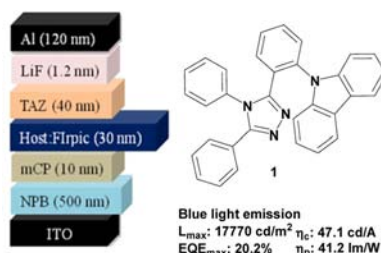
Man-kit Leung,<sup>\*,†,‡</sup> Yu-Hsuan Hsieh,<sup>†</sup> Ting-Yi Kuo,<sup>†</sup> Pi-Tai Chou,<sup>†</sup> Jiun-Haw Lee,<sup>§</sup> Tien-Lung Chiu,<sup>\*,||</sup> and Hsin-Jen Chen<sup>||</sup>

Department of Chemistry, Institute of Polymer Science and Engineering, Department of Electrical Engineering and Graduate Institute of Photonics and Optoelectronics, National Taiwan University, 1 Roosevelt Road Section 4, Taipei 106, Taiwan, R.O.C., and Department of Photonics Engineering, Yuan Ze University, 135 Yuan-Tung Road, Chung-Li 32003, Taiwan, R.O.C.

mkleung@ntu.edu.tw; tlchiu@saturn.yzu.edu.tw

Received July 17, 2013

## ABSTRACT



Ambipolar triplet hosts comprising 1,2,4-triazole and carbazole in ortho-positions have been developed. The blue PHOLED has a high current efficiency of  $47.1 \text{ cd A}^{-1}$ , power efficiency of  $41.2 \text{ lm W}^{-1}$ , and low efficiency roll-off. The high efficiency was attributed to the successful control of  $\pi$ -conjugation through orthogonal arrangement of the substituents so that a wide  $T_1$ – $S_0$  gap could be maintained.

Organic light-emitting diodes (OLEDs) have high potential in full-color flat-panel displays and lighting applications.<sup>1</sup> Phosphorescent organic light-emitting diodes (PHOLEDs) are particularly attractive because their theoretical quantum efficiency can be, in principle, four times higher than that of the fluorescent based OLEDs.<sup>2</sup> However, high efficiency blue-light-emitting PHOLEDs are difficult to achieve due to the high-lying triplet state requirement that usually leads to low emission efficiency and a short device lifetime. In addition, host matrices are required so that phosphorescent emitters can be dispersed homogeneously into a suitable

organic host, and with this strategy, a detrimental effect such as aggregation quenching and triplet–triplet annihilation of phosphors can be suppressed. Good host materials should meet some requirements: (i) higher triplet  $T_1$  energy to prevent exothermic reverse energy transfer (ET) from the emitters and hence confine triplet excitons within the emitting layer,<sup>3</sup> (ii) suitable HOMO/LUMO levels to lower the interfacial energy barriers between its neighboring active layers,<sup>4</sup> and (iii) balanced charge transport properties to restrict the electron–hole recombination within the emitting layer and thus reduce the efficiency roll-off.<sup>5</sup> Recent research emphasizes the use of ambipolar hosts to keep the charge-transport balanced.<sup>6</sup> The challenge is to incorporate electron-donating

<sup>†</sup> Department of Chemistry, National Taiwan University.

<sup>‡</sup> Institute of Polymer Science and Engineering, National Taiwan University.

<sup>§</sup> Department of Electrical Engineering and Graduate Institute of Photonics and Optoelectronics, National Taiwan University.

<sup>||</sup> Yuan Ze University.

(1) Tang, C. W.; VanSlyke, S. A. *Appl. Phys. Lett.* **1987**, *51*, 913.

(2) (a) Baldo, A.; O'Brien, D. F.; You, Y.; Shoustikov, A.; Sibley, S.; Thompson, M. E.; Forrest, S. R. *Nature* **1998**, *395*, 151. (b) Jeon, S. O.; Lee, J. Y. *J. Mater. Chem.* **2012**, *22*, 4233. (c) Yook, K. S.; Lee, J. Y. *Adv. Mater.* **2012**, *24*, 3169. (d) Jeon, S. O.; Jang, S. E.; Son, H. S.; Lee, J. Y. *Adv. Mater.* **2011**, *23*, 1436.

(3) (a) Padmaperuma, A. B.; Sapochak, L. S.; Burrows, P. E. *Chem. Mater.* **2006**, *18*, 2389. (b) Su, S.-J.; Sasabe, H.; Takeda, T.; Kido, J. *Chem. Mater.* **2008**, *20*, 169.

(4) Lu, M. H.; Weaver, M. S.; Zhou, T. X.; Rothman, M.; Kwong, R. C.; Hack, M.; Brown, J. J. *Appl. Phys. Lett.* **2002**, *81*, 3921.

(5) (a) Chaskar, A.; Chen, H.-F.; Wong, K.-T. *Adv. Mater.* **2011**, *23*, 3876. (b) Tao, Y.; Yang, C.; Qin, J. *Chem. Soc. Rev.* **2011**, *40*, 2943. (c) Duan, L.; Qiao, J.; Sun, Y.; Qiu, Y. *Adv. Mater.* **2011**, *23*, 1137.

(6) Su, S. J.; Cai, C.; Kido, J. *Chem. Mater.* **2011**, *23*, 274.

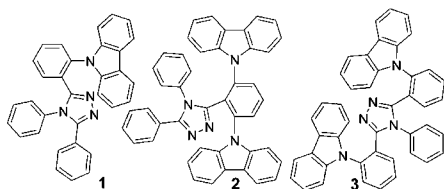


**Figure 1**

and -withdrawing moieties into one molecule without creating strong donor–acceptor interactions so that the low triplet energy ( $E_T$ ) states caused by intramolecular charge transfer (CT) can be avoided. Many successful designs<sup>7</sup> with typical linking groups such as diphenylsilane<sup>8</sup> and diphenylphosphine oxide<sup>9</sup> have been used.

1,2,4-Triazoles (Tazs) and carbazoles (Cbzs) are common electron-transporting and donating high triplet host materials for PHOLEDs. In the present work, ambipolar hosts **1–3** (Figure 1) comprising Taz and Cbz moieties and bridged with an *ortho*-substituted benzene ring have been developed and studied.

**Synthesis.** Nucleophilic aromatic substitution of **4** with 9*H*-carbazole led to **5** (87%) (Scheme 1).<sup>10</sup> Condensation of **5** with aniline, using  $\text{AlCl}_3$  as a Lewis acid catalyst as well as a dehydrating agent, gave **1** (58%).<sup>11</sup> Under similar conditions, **6** and **7** were converted to the corresponding *N*-phenyltriazole intermediates, followed by nucleophilic aromatic substitution to give **2** (79%) and **3** (70%), respectively.

(7) (a) Hung, W. Y.; Tu, G. M.; Chen, S. W.; Chi, Y. *J. Mater. Chem.* **2012**, *22*, 5410. (b) Rothmann, M. M.; Fuchs, E.; Schildknecht, C.; Langer, N.; Lennartz, C.; Munster, I.; Strohrriegel, P. *Org. Electron.* **2011**, *12*, 1192. (c) Su, S. J.; Cai, C.; Takamatsu, J.; Kido, J. *Org. Electron.* **2012**, *13*, 1937. (d) Zhuang, J.; Su, W.; Li, W.; Zhou, Y.; Shen, Q.; Zhou, M. *Org. Electron.* **2012**, *13*, 2210. (e) Chen, H. F.; Chi, L. C.; Hung, W. Y.; Chen, W. J.; Hwua, T. Y.; Chen, Y. H.; Chou, S. H.; Mondal, E.; Liu, Y. H.; Wong, K. T. *Org. Electron.* **2012**, *13*, 2671. (f) Lee, C. W.; Lee, J. Y. *Org. Electron.* **2013**, *14*, 1602. (g) Lee, C. W.; Kim, J.-K.; Joo, S. H.; Lee, J. Y. *ACS Appl. Mater. Interfaces* **2013**, *5*, 2169. (h) Lee, C. W.; Lee, J. Y. *Chem. Commun.* **2013**, *49*, 1446. (i) Swensen, J. S.; Polikarpov, E.; Von Ruden, A.; Wang, L.; Sapochak, L. S.; Padmaperuma, A. B. *Adv. Funct. Mater.* **2011**, *21*, 3250. (j) Hua, D. h.; Cheng, G.; Li, H.; Lv, Y.; Lu, P.; Ma, Y. g. *Org. Electron.* **2012**, *13*, 2825. (k) Peng, T.; Yang, Y.; Bi, H.; Liu, Y.; Hou, Z. m.; Wang, Y. *J. Mater. Chem.* **2011**, *21*, 3551. (l) Zhao, X.-H.; Zhang, Z.-S.; Qian, Y.; Yi, M.-D.; Xie, L.-H.; Hu, C.-P.; Xie, G.-H.; Xu, H.; Han, C.-M.; Zhao, Y.; Huang, W. *J. Mater. Chem. C* **2013**, *1*, 3482. (m) Wada, A.; Yasuda, T.; Zhang, Q. s.; Yang, Y. S.; Takasu, I.; Enomoto, S.; Adachi, C. *J. Mater. Chem. C* **2013**, *1*, 2404. (n) Xia, Z.-Y.; Zhang, Z.-Y.; Su, J.-H.; Zhang, Q.; Fung, K.-M.; Lam, M.-K.; Li, K.-F.; Wong, W.-Y.; Cheah, K.-W.; Tian, H.; Chen, C. H. *J. Mater. Chem.* **2010**, *20*, 3768.

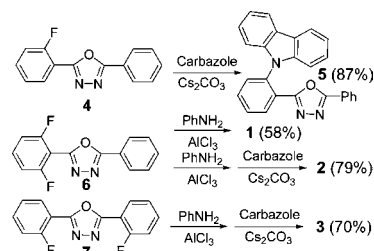
(8) (a) Leung, M. k.; Yang, W. H.; Chuang, C. N.; Lee, J. H.; Lin, C. F.; Wei, M. K.; Liu, Y. H. *Org. Lett.* **2012**, *14*, 19. (b) Holmes, R. J.; D'Andrade, B. W.; Forrest, S. R.; Ren, X.; Li, J.; Thompson, M. E. *Appl. Phys. Lett.* **2003**, *83*, 3818. (c) Ren, X.; Li, J.; Holmes, R. J.; Djurovich, P. I.; Forrest, S. R.; Thompson, M. E. *Chem. Mater.* **2004**, *16*, 4743.

(9) (a) Chou, H. H.; Cheng, C. H. *Adv. Mater.* **2010**, *22*, 2468. (b) Chang, H. H.; Tsai, W. S.; Chang, C. P.; Chen, N. P.; Wong, K. T.; Hung, W. Y.; Chen, S. W. *Org. Electron.* **2011**, *12*, 2025. (c) Jiang, W.; Duan, L.; Qiao, J.; Dong, G. f.; Wang, L.d.; Qiu, Y. *Org. Lett.* **2011**, *13*, 3146.

(10) Kawano, T.; Yoshizumi, T.; Hirano, K.; Satoh, T.; Miura, M. *Org. Lett.* **2009**, *11*, 3072.

(11) Chiriac, C. I.; Tanasa, F.; Nechifor, M. *Rev. Roum. Chim.* **2010**, *55*, 175.

**Scheme 1**



**Crystallographic Analysis.** X-ray crystallography is useful for understanding material properties.<sup>12</sup> Figure 2 shows the ORTEPs of **1**, **2**, and **3**. Due to steric repulsions between the Taz and the Cbz moieties, these substituents possess noncoplanar alignment to the central benzene ring with the dihedral angles (DAs) mainly larger than 45° so that the  $\pi$ -conjugations are interrupted. However, the close distances between the Taz and Cbz groups still allow effective through-space  $\pi$ -interactions.

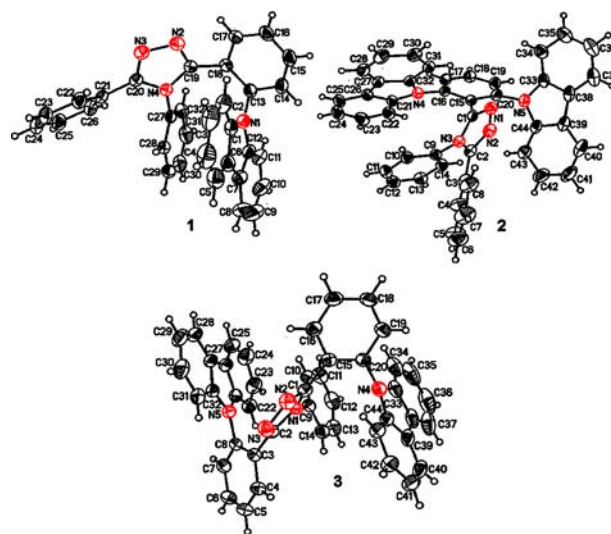


**Figure 2.** ORTEPs of **1–3**.

A single crystal of **1** clearly shows that the *N*-phenyl group on the Taz segment and the Cbz ring are face-to-face aligned. Both groups are rotated with respect to the central benzene ring, and the DAs 53.5° for C1–N1–C13–C18 and 51.9° for N2–C19–C18–C17 were recorded. The short estimated centroid distance of 3.67 Å strongly suggests through-space electronic  $\pi$ – $\pi$  interactions. Similar conformational preferences were found in **2** and **3**. In **2**, the DAs 43.1° and 67.4° for the carbazole rings were found. The sandwiched Taz unit is kept at a

(12) (a) Zhou, G.-j.; Wang, Q.; Ho, C.-L.; Wong, W.-Y.; Ma, D.-g.; Wang, L.-x.; Lin, Z.-y. *Chem. Asian J.* **2008**, *3*, 1830. (b) Zhou, G.-j.; Ho, C.-L.; Wong, W.-Y.; Wang, Ma, Q., D.; Wang, L.-x.; Lin, Z.-y.; Marder, T. B.; Beeby, A. *Adv. Funct. Mater.* **2008**, *18*, 499.

**Table 1.** Physical Properties of **1–3**

	UV–vis ( $\lambda_{\text{max}}$ , nm)	FL ( $\lambda$ , nm)	Ph ( $\lambda$ , nm)	$E_{\text{T}}$ (eV)	$E_{\text{g}}$ (eV)	$E_{\text{ox}}^{\text{onset}}$ (V)	$E_{\text{red}}^{\text{onset}}$ (V)	HOMO/ LUMO (eV)	$T_{\text{g}}$ (°C)	$T_{\text{d}}$ (°C)
<b>1</b>	286	395, 341/358	451	3.09	3.44	–2.22	1.22	–5.7/–2.3	87	349
<b>2</b>	286	403	442	3.07	3.34	–2.15	1.19	–5.7/–2.3	–	365
<b>3</b>	290	395, 342/358	443	3.09	3.40	–2.21	1.20	–5.7/–2.3	–	353

large DA of 60.1° to the benzene linker group. In **3**, the *N*-phenyl group on the Taz segment is parallel displaced with the Cbz rings and with centroid short distances of 3.74 and 3.84 Å being measured. The DAs 54.2° for C(7)–C(8)–N(5)–C(21), 47.4° for C(19)–C(20)–N(4)–C(33), 60.4° for N(3)–C(2)–C(3)–C(4), 52.6° for N(2)–C(1)–C(15)–C(16), and 55.9° for C(1)–N(1)–C(9)–C(10) were recorded. Again, all the DAs were found to be >45°, indicating orthogonal alignments of the aromatic units. This will be beneficial for maintaining the  $T_1$  states (the lowest triplet state) at high energy levels.

**Photophysical Properties.** Compounds **1–3** show strong absorptions below 300 nm that are attributed to the  $\pi$ – $\pi^*$  transitions of the Taz and Cbz chromophores (Table 1 and Figure 3). The absorptions that ranged 300–350 nm with ample vibronic patterns are characteristic for the Cbz chromophore that is nearly identical to that of *N*-phenylcarbazole (NPC).<sup>13</sup> The presence of the Taz group in **1–3** does not introduce any significant electronic perturbations or red shift to the absorption spectra of the carbazole moiety. This may be due to the nonconjugative orthogonal alignment of the aromatic units, which were confirmed in the crystallographic analysis, that allows the substituents to function as independent chromophores.

**Room-Temperature Photoluminescence (PL).** Compounds **1** and **3** strongly fluoresce to give dual emissions at 325–535 nm that are well overlapped with the MLCT absorption of FIrpic, allowing ET from **1–3** to FIrpic. The first emission of **1** and **3** shows the vibronic fine pattern peaked at 341 and 358 nm, with a reasonably small Stokes shift of 8 nm. The emission pattern is nearly identical to that of NPC, suggesting that this emission is governed by the Cbz fluorophore. The second emission peaking at 395 nm shows typical CT character; the emissions are broad and structureless with the intensity solvent polarity dependent. On the other hand, formation of the CT state is extremely effective for **2** so that the CT emission dominates in its photoemission. The dual-emission phenomena were further confirmed by time-dependent fluorescence-decay experiments. For example, the transient spectra of **1** (Figure 3d) show a decay lifetime of 1.19 ns at 340 nm and a rise time of 0.94 ns followed by a decay lifetime of 2.23 ns at 450 nm. Furthermore, the excitation spectra of **1** about  $\lambda = 360$  and 450 nm superimpose with each other perfectly, supporting the hypothesis of dual-emission properties from the same species; the short lifetime and the superimposition in

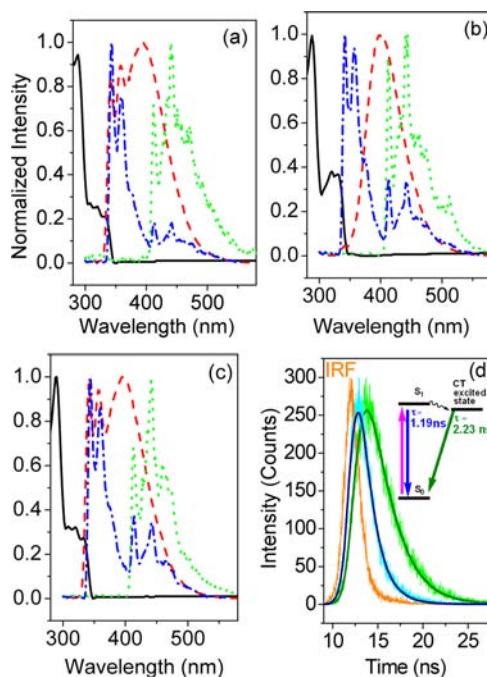


**Figure 3.** UV–visible, fluorescence, low temperature fluorescence, and low temperature phosphorescence spectra of (a) **1**; (b) **2**; (c) **3**, and (black) UV; (red) FL; (green) Ph; (blue) LTFL. (d) Transient spectra of **1** at  $\lambda = 340$  (blue) and 450 nm (green) in the time-dependent fluorescence decay experiments with excitation at 310 nm (orange: instrument response function; blue: emission at 340 nm,  $\tau = (+)$  1.19; green: emission at 450 nm,  $\tau = (+)$  2.23 (–) 0.94.

excitation spectrum indicate that the CT emission may be an intramolecular process with the same ground state.

**Low Temperature PL Behavior.** The second CT emission band disappears in the PL spectra in THF organic glass at 77 K, and only emission from the carbazole unit could be detected. This may probably due to two reasons: (1) Formation of the CT excited state requires conformational change from the initial  $S_1$  state that could be inhibited by restricted rotation in the organic glass. (2) Stabilization of the CT excited state through dipole–dipole interactions requires solvent orientation relaxation that is prohibited at low temperature in the organic glassy matrix. The low temperature phosphorescence spectra of **1–3** and NPC are almost identical with similar  $E_{\text{T}}$  levels of 3.00–3.09 eV that were recorded but significantly different from that of 3,4,5-triphenyl-1,2,4-triazole (TPT). This observation suggested that the triplet state is confined at the carbazole

(13) Lee, C. C.; Leung, M.-k.; Lee, P.-Y.; Chiu, T.-L.; Lee, J.-H.; Liu, C.; Chou, P.-T. *Macromolecules* **2012**, *45*, 751.



**Table 2.** Performances of PHOLED Devices 1–3

device <sup>a</sup>	$L_{\max}^b$ (cd/m <sup>2</sup> )	$\eta_{c,\max}^c$ (cd/A)	$\eta_{p,\max}^d$ (lm/W)	EQE <sub>max</sub>	CIE shift $\Delta x, \Delta y$
1, 15%	17 770	47.1	41.2	20.2%	0.016, 0.043
2, 12%	17 510	43.3	38.6	17.9%	0.016, 0.039
3, 9%	15 730	40.2	36.1	17.1%	0.013, 0.031

<sup>a</sup> Host-FIrpic doping level. <sup>b</sup> At 12 V. <sup>c</sup>  $E_{\text{applied}}$  for 1, 2, and 3 are 4, 4, and 3.5 V. <sup>d</sup> At 3.5 V.

unit. The  $E_T$  is obviously higher than that of FIrpic (2.65 eV),<sup>3b</sup> implying that 1–3 are potential host materials for blue-light triplet emitters.

**Electrochemical Properties.** The ambipolar behaviors of 1–3 ( $10^{-3}$  M) were evaluated by cyclic voltammetry (See Table 1 and SI). Regardless of the structural differences, 1–3 show similar redox behavior. In the anodic scans, 1–3 show irreversible oxidation on the Cbz ring with nearly the same  $E_{\text{onset}}$  at 1.2 V. In the cathodic scans, the irreversible reduction on the Taz unit was observed at  $E_{\text{onset}} = -2.2$  V (Table 1). These results again indicated that electronic couplings between the Cbz units and the Taz units are minimal and can be considered more or less as nonconjugated ones.

**Electroluminescence Performances.** The electronic properties of 1–3 were examined by the hole- and electron-only methods<sup>14</sup> (see SI). The discrepancy of the hole and electron currents is within 1 order of magnitude, strongly suggesting that 1–3 are ambipolar materials. The PHOLED performance was evaluated on a device of ITO/NPB/mCP/FIrpic in 1, 2, or 3/TAZ/LiF/Al (Table 2), in which TAZ is 3-(4-biphenyl)-4-phenyl-5-*tert*-butylphenyl-1,2,4-triazole and NPB is *N,N'*-diphenyl-*N,N'*-bis(1-naphthyl)(1,1'-biphenyl)-4,4'-diamine. The high HOMO–LUMO gap of 3.34–3.44 eV and  $E_T$  of 3.07–3.09 eV for 1–3 enable the intermolecular ET from 1–3 to FIrpic (2.65 eV). Thus, all the PHOLED exhibited a main emission peak at 472 nm, which is typical for FIrpic-containing devices with hosts. The PHOLED performance was FIrpic doping-level dependent. Maximum luminescence ( $L_{\max}$ ) of 19 160, 17 510, and 16 720 cd/m<sup>2</sup> was achieved at 12 V for 1, 2, and 3, with FIrpic doping levels of 18, 12, and 15 wt % being adopted respectively. Since the triplet–triplet annihilation effect may occur at high concentration, we optimized the FIrpic doping levels so that 1 (15 wt %), 2 (12 wt %), and 3 (9 wt %) are found for obtaining the highest current efficiency ( $\eta_c$ ) of 47.1 (4 V), 43.3 (4 V), and 40.2 cd/A (3.5 V); power efficiency ( $\eta_p$ ) of 41.2, 38.6, and 36.1 lm/W at 3.5 V; and external quantum efficiency (EQE<sub>max</sub>) of 20.2%, 17.9%, and 17.1%.

(14) Chu, T. Y.; Song, O. K. *Appl. Phys. Lett.* **2007**, *90*, 203512.

(15) Eom, S.-H.; Zheng, Y.; Wrzesniewski, E.; Lee, J.; Chopra, N.; So, F.; Xue, J. *Org. Electron.* **2009**, *10*, 686.

(16) Wei, M.-K.; Lin, H.-Y.; Lee, J.-H.; Chen, K.-Y.; Ho, Y.-H.; Lin, C.-C.; Wub, C.-F.; Lin, H.-Y.; Tsai, J.-H.; Wu, T.-C. *Opt. Commun.* **2008**, *281* (2008), 5625.

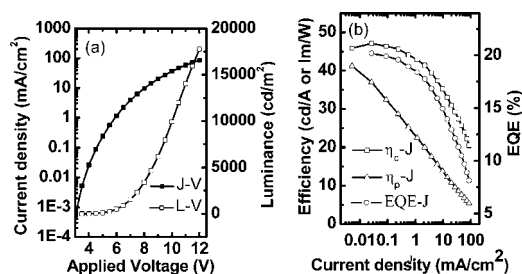
**Figure 4.** PHOLED device properties of 1: (a) Voltage–current–brightness plots; (b) Efficiency plots.

Figure 4 shows the voltage–current–brightness and the current density–efficiency plots of the resultant device for 1. Although rolling-off of the efficiency for PHOLED is commonly observed at high driving currents due to triplet–triplet annihilation, the current efficiency ( $\eta_c$ ) at 100 and 1000 cd/m<sup>2</sup> remains high in the present cases. The comparably high  $\eta_c$  of 46.3, 42.3, and 38.8 cd/A for the resultant devices of 1, 2, and 3 at 100 cd/m<sup>2</sup> and 41.1, 39.5, and 35.7 cd/A at 1000 cd/m<sup>2</sup> were recorded respectively. The blue color stability is outstanding. The CIE (Commission International de L'Eclairage) of (0.16, 0.38) at 6 V for all the devices, with only small CIE coordinate shifts, were recorded upon variation of the applied electrical voltage in the range 3.5–12 V.

In conclusion, we report a simple design of ambipolar hosts 1–3 for FIrpic that leads to high luminescence  $\eta_c$ , low efficiency roll-off, and high color stability. Without adopting any high performance carrier-blocking materials such as 1,1-bis-(4-bis(4-methylphenyl)aminophenyl)-cyclohexane (TAPC), hole-blocking material such as 1,4-bis(triphenylsilyl)benzene (UGH-2),<sup>8b</sup> or electron-transport materials such as tris[3-(3-pyridyl)mesityl]borane (3TPYMB),<sup>15</sup> or by any special technique such as microlens for light extraction,<sup>16</sup> significantly high efficiency for the resultant devices of 1, 2, and 3 were obtained. The high efficiency was attributed to the successful control of the degree of conjugation in the host molecules through orthogonal arrangement of the substituents so that a wide  $T_1$ – $S_0$  gap could be maintained.

**Acknowledgment.** We are thankful for financial support from NSC-101-2113-M-002-010-MY3, NSC-102-2622-E-155-008-CC3, 102-EC-17-A-08-S1-183, and to Mr. Jau-Jiun Huang for the energy transfer measurements.

**Supporting Information Available.** NMR, DSC, TGA, CV, CIF, HOMO/LUMO, and OLED data. This material is available free of charge via the Internet at <http://pubs.acs.org>.

The authors declare no competing financial interest.